Visible Spectroscopy

Mitchell Kelly* and Tristen Jensen
University of Florida Department of Physics
(Dated: March 10, 2023)

The discrete energy levels described by the Bohr model of the atom, allow for electrons to emit photons while transitioning to a level of lower energy. The Balmer series set of visible light wavelengths characteristic of certain gasses' emission spectrum can analyzed using a gas discharge lamp and transmission grating spectrometer apparatus. Fitting helium calibration data with linear regression allowed for the calculation of the groove spacing, which was approximately the manufacturer's value of 1657.29 lines/nm with an uncertainty of 0.24 lines/nm. The fitted constants of the regression were used to verify the visible emission lines of hydrogen while calculating the reduced mass Rydberg constant at 109722.8 cm^{-1} with an uncertainty of 29.8 cm^{-1}. χ^2 regression analysis was conducted for the fits of helium calibration and hydrogen wavelength determination with the resultant χ^2 no greater than a σ_{χ^2} amount lower than the degrees of freedom.

1. INTRODUCTION AND THEORY

The simplistic quantum-mechanical model of an electron orbiting a proton, coined the Bohr model of the atom, assumes that quantized angular momentum values lead to discrete energy levels depending on, $n = 1, 2, \ldots$, a positive integer [1]. The angular momentum defined by $L = n\hbar$, where $\hbar = h/2\pi$ is the reduction of Planck's constant h, depends explicitly on this principal quantum number n. This system's energy levels are expressed by

$$E_n = -\frac{\mu e^4}{8\epsilon_0^2 h^2 n^2} \tag{1}$$

where e is the charge of an electron, ϵ_0 is the permittivity of free space, and μ equals the reduced mass of the proton-electron system $\frac{m_e m_p}{m_e + m_p}$ [1].

Whenever the electron transitions from a higher energy level to a lower energy level a photon is emitted at a wavelength $\lambda = hc/\Delta E$ where $\Delta E = E_{n_i} - E_{n_f}$ is the excess energy of this photon dropping from the initial energy state to the final energy state [1]. The wavelengths of such photons comprising the emission spectrum of Hydrogen are predicted by the equation

$$\frac{1}{\lambda} = R_H \left(\frac{1}{n_f^2} - \frac{1}{n_i^2} \right) \tag{2}$$

where

$$R_H = \frac{\mu e^4}{8\epsilon_0^2 h^3 n^2} \tag{3}$$

is the reduced mass Rydberg. It should be noted that Eq. 3 has an infinite proton mass counterpart known as the infinite mass Rydberg defined below.

$$R_\infty = \frac{m_e e^4}{8\epsilon_0^2 h^2 n^2} \tag{4}$$

When n_f is fixed at 2, the Balmer series is observed, exhibiting visible light as $n_i = 3, 4, \ldots$ increases. A properly calibrated transmission grating spectrometer can precisely measure these emission lines of low atomic number elements. Furthermore, the spectral lines seen in hydrogen are observed to be split into two closely-spaced lines from the fine structure of the atom if the resolution is great enough. The splitting is caused by the electron's spin as it orbits the nucleus, and a much smaller "hyperfine" splitting derived from the nucleus's interactions with the electron's electric field also exist. In most cases these are difficult to resolve since the energy transition is much greater than the splitting energy where their fraction is $\approx 1/42{,}000$.

The wavelength of light observed from the emission spectrum is determined from the scattering of waves from the grooves of a transmission grating, where the diffraction order m $(0, \pm 1, \pm 2, \ldots)$ is a product of wavelength λ.

$$m\lambda = d(\sin\theta_r - \sin\theta_i) \tag{5}$$

The grating groove spacing is defined as d, and the incident angle θ_i and diffraction angle θ_r are relative to the grating normal [1]. The diffraction order is positive whenever the diffraction angle is larger than the incident angle, negative whenever the diffraction angle is smaller than the incident angle, and zero when both are equal.

Mentioned previously, resolution refers to the ability of a spectrometer to separate two closely located spectral lines [1]. According to the resolving power formula,

$$\frac{\lambda}{\Delta\lambda} = mN \tag{6}$$

the spectral lines will begin to overlap a tiny separation $\Delta\lambda$ where the Rayleigh criterion defines that as the "just resolvable" wavelength difference [1]. The fraction in Eq. 6 represents the resolving power while N is the number of grooves observed at that specific resolving power. Additionally, at higher dispersion, $(d\theta_r/d\lambda)$, the spectral lines are spaced farther apart, where θ_r is the angle at which the spectrometer telescope measures the position of the spectral line.

*Electronic address: mitchellkelly@ufl.edu

2. APPARATUS AND EXPERIMENT

The emission spectra of helium and hydrogen come from their gaseous state contained in a gas discharge tube where the energy level transitions of electrons in the gas emit light in the visible part of the spectrum [2]. A gas discharge lamp applies a current between the two electrodes of a gas discharge tube where the cathode emits electrons into the gas and the anode collects electrons [2]. Helium and hydrogen atoms are subsequently put into excited states, and afterward electrons lose energy in the form of a photon when they transition back from the excited state.

In order for the spectrometer to observe the emission spectrum of helium and hydrogen via diffraction off of the transmission grating, it needs to be properly aligned. The three main components of the semi-precision instrument are the telescope, collimator, and transmission grating's table seen in Figure 1 top down. The telescope takes parallel rays of light (created from collimator), and after diffraction occurs on the grating where θ_r is adjusted to line up the telescope's reticle onto the spectral lines.

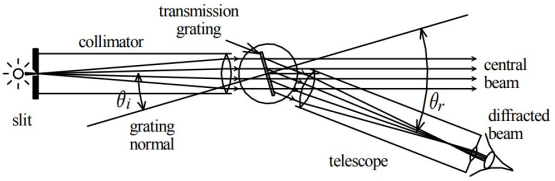

FIG. 1: Schematic diagram of spectrometer internals where light ray paths are illustrated while grating and telescope angles are defined.

The telescope was first aligned to an object at infinity where the cross hair and object were simultaneously in focus without any parallax. With the telescope focus kept the same, the entrance slit of the collimator was adjusted horizontally and narrowed to desired width, and the collimator tube was altered until the slit was in sharp focus. Once the telescope's leveling screws were adjusted and the reticle remained centered on the slit, the transmission grating was mounted onto its table. By rotating the telescope to make a 90° angle with the collimator and ensuring proper grating alignment, a reflection of the collimator slit was observed. It ensured the grating normal was perpendicular to the telescope's main rotation axis. Autocollimation was achieved by shining light into the small hole on the side of the telescope with the telescope itself rotated half-way to the collimator. Afterward, the table with the grating attached was fully removed and similar adjustments of the focus on infinity and the slit were conducted again to make the collimator's axis perpendicular to the main rotation axis [1]. The table was reattached to the spectrometer where a rough angle of incidence of $\approx$ 5-10° was established. Finally, the grating dispersion plane was adjusted with its leveling screws so that diffracted light "rainbows" were seen. The spectrometer became fully adjusted and aligned, so measurements of spectral lines with relation to Eq. 5 could be conducted.

Calibration measurements of the known wavelengths of spectral lines were conducted to determine the grating groove spacing, and to verify the initial incidence and normal angle readings were accurate. These fitted calibration parameters were then used to estimate the value of the reduced mass Rydberg (Eq. 3) by direct application of Eq. 5 for first and second order images of hydrogen's spectral lines. At all diffraction angles θ_r a measurement of A_r and B_r are recorded, where A and B correspond to two vernier scales approximately spaced 180◦ apart. Each A_r and $B_r \pm 180$ are averaged into a single H_r which was the angle used primarily in the analysis. The uncertainty of these angular measurements, σ_r, was estimated as 1 minute of arc for helium measurements and 3 minutes of arc for hydrogen measurements.

Utilizing a sodium lamp in a separate investigation, the sodium doublet lines of 589.0 nanometers and 589.6 nanometers respectively were also studied to highlight Eq. 6's properties in relation to an adjustable auxiliary slit placed on the opposite end of the collimator.

Systematic errors with the spectrometer can arise from improper calibration: slight parallax, issues with the focus of the reticle, and imperfect autocollimation. All measured A_r and B_r would then be less accurate than a perfectly calibrated spectrometer if any one of the previous mistakes occurred. Any random error was a direct result of how the vernier scale measurements required discernment by the unaided eye. Head positioning and light level can play a role what value is deemed to be a correct measurement. Even with the average of both lab partner's reading considered, measurements could differ substantially which directly impacted the value of σ_r needed for that particular measurement.

3. ANALYSIS AND RESULTS

A weighted linear regression with calibration uncertainty was achieved by fitting the H_r angles of helium measurements to the grating fit equation,

$$m\lambda = D_s \sin H_r + D_c \cos H_r + D_0 \tag{7}$$

where D_s, D_c, and D_0 are the fitting parameters. See Appendix A for a proof of Eq. 7 derived from Eq. 5 with the fitting parameters defined accordingly. The uncertainty in $m\lambda$ due to the uncertainty in H_r ($\sigma_{m\lambda} = |\partial(m\lambda)/\partial H_r|\sigma_r$) was calculated to form the weighting matrix $[\sigma^2_{m\lambda}]^{-1}$ which facilitated the proper linear regression fit. A 3 by 1 column vector of the fitting parameters was created using matrix multiplication of the parameter covariance matrix ($[\sigma^2_b]$) with the transpose of the Jacobian ($[J^{m\lambda}_b]^T$), the weighting matrix, and the reference

helium wavelengths ($m\lambda$). With utilization of the Jacobian in terms of measured H_r, the fitting parameters were determined for the the setup's specific orientation and experimentally chosen angle of incidence.

D_0, D_s, and D_c were determined to be -269.85, -1442.13, and 816.62 respectively with an uncertainty of 0.37, 0.40, and 0.30 for each of them (all in lines/nm). The grating spacing d was calculated from $\sqrt{D_s^2 + D_c^2}$ where it was valued at 1657.29 lines/nm with an uncertainty of 0.236 lines/nm, approximately the manufacturer's specification of 1 line per 600 mm. A χ^2 of 8.39 was calculated regarding the fit to Eq. 7, and it barely stayed within 1 sigma (σ_{χ^2}) of 13 degrees of freedom in the χ^2 test. Thus, the calibration fit of helium wavelengths matched the data appropriately in regard to the theory of Eq. 5.

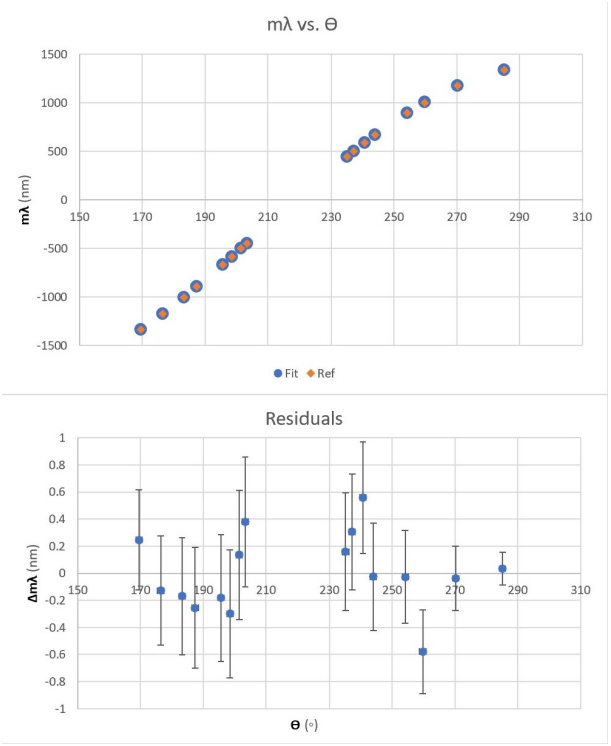

FIG. 2: Plot of $m\lambda$ versus H_r (θ) for helium calibration with residuals $\Delta m\lambda$ of the difference between reference and fit-calculated $m\lambda$.

Figure. 2 illustrates the fitted $m\lambda$ and helium reference $m\lambda$ with their residuals and corresponding error bars of the weighted $\pm\sigma_{m\lambda}$ uncertainty of each measurement.

After the fitting parameters of Eq. 7 were determined with the helium calibration data analysis, a new Jacobian of the hydrogen H_r angles was created to determine the specific $m\lambda$ for hydrogen emission lines. The equation, $\mathbf{m\lambda} = [J_b^{m\lambda}]\mathbf{b}$, determined $m\lambda$ for each measurement, and the wavelength was traced back knowing the image order of the hydrogen measurement. Note that $\mathbf{b}$ is the column vector of the fitting parameters. With these new wavelengths, the fit of the Rydberg formula (Eq. 2) required a new weighting matrix $[\sigma_{1/\lambda}^2]^{-1}$ where $\sigma_{1/\lambda} = |(1/m\lambda^2)(\partial(m\lambda)/\partial H_r)|\sigma_r$.

The reduced mass Rydberg constant (Eq.3) abbreviated R was calculated from, $R = [J_{1/\lambda}^R]^\dagger \mathbf{y}$, where $[J_{1/\lambda}^R]^\dagger$ is the weighted Moore-Penrose pseudo-inverse of $[J_R^{1/\lambda}]$ $(1/n_f^2 - 1/n_i^2)$, and $\mathbf{y}$ is the column vector of $1/\lambda$. The pseudo-inverse

$$[J_{1/\lambda}^R]^\dagger = [\sigma_R^{2(r)}][J_R^{1/\lambda}]^T[\sigma_{1/\lambda}^2]^{-1}$$

and the covariance matrix of R due to uncertainty in H_r

$$[\sigma_R^{2(r)}] = [[J_R^{1/\lambda}]^T[\sigma_{1/\lambda}^2]^{-1}[J_R^{1/\lambda}]]^{-1}$$

are both essential components to the determination of the reduced mass Rydberg constant.

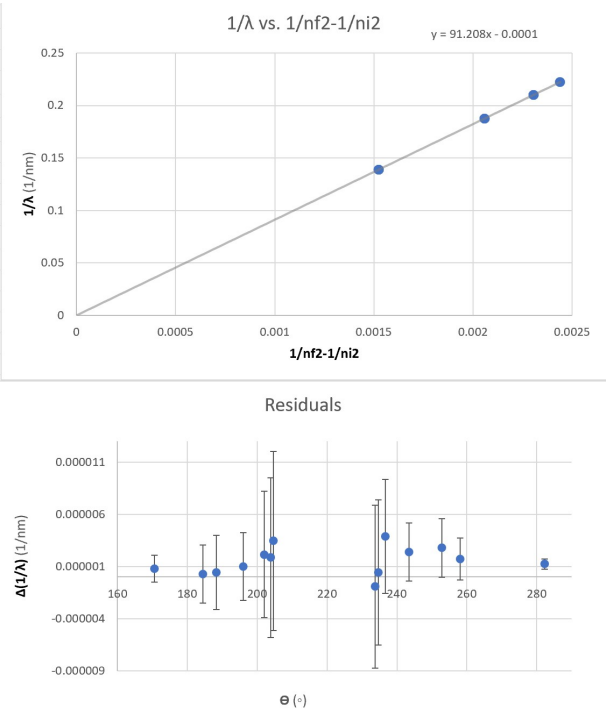

FIG. 3: Plot of $m\lambda$ versus H_r (θ) for hydrogen with residuals $\Delta m\lambda$ of the difference between the fit calculated inverse wavelength and reference inverse wavelengths.

From the formulas described above, R_H was calculated to be 109772.8 cm^{-1} with an uncertainty of 29.82 cm^{-1}, and the official high-accuracy value of R_H comes in at 109677.5 cm^{-1}. Additionally, the variance of R_H due to uncertainties of H_r was tabulated to be 2.88 x 10^{-6} nm^{-1}, and the uncertainty in R_H due to the uncertainty in the calibration parameters was calculated to be 7.64 x 10^{-7} nm^{-1}. Figure. 3 illustrates the fit between the calculated and referenced hydrogen wavelengths and their corresponding residuals determined from the modified weighting function. According to the theory, the top graph of Figure. 3 should have a y-intercept of 0, and

a linear relationship between the variables is exhibited with a y-intercept of ≈ 0. The fit analysis revealed a χ^2 of 9.99 which is within the 1 (σ_{χ^2}) range of 13 degrees of freedom.

The value of the reduced mass Rydberg produced from the Rydberg fit tests the difference between the official infinite mass Rydberg and the reduced mass Rydberg because it falls between $\pm R_h - R_\infty$. Additionally, the uncertainty in the measurement is smaller than the difference between the two, meaning the uncertainty is small enough to differentiate between both values instead of being unable to tell which one is pertinent to the investigation.

Observing the sodium doublet lines with an extremely narrow entrance slit, the vertically oriented auxiliary slit width was 0.9mm, per measurement with calipers. By narrowing the auxiliary slit width until the doublet lines reached their minimum "just resolvable" $\Delta\lambda$, Eq. 6 must be considered, and the number of grooves illuminated decreases likewise. N is equal to the fraction of slit width and groove spacing d, so N was calculated as approximately 543.15 lines. While viewing the doublet in second order at the same auxiliary slit width the lines became resolvable. N and m are proportional in Eq. 6, so when second order lines are being observed, it takes half the resolving power to resolve the same amount. Therefore, the slit would have to become even narrower so N decreases and hits the new limit of minimum resolving power.

4. CONCLUSIONS

It was proven that transmission gratings can disperse the emission spectra of helium and hydrogen according to Eq. 5, and their visible light can be accurately distinguished using a spectrometer. The results for Helium calibration wavelengths were accurate enough to be able to predict the Rydberg constant of Eq. 2. Across all measurements and calculations the uncertainty in H_r did not significantly affect the results nor prevent the fundamental theory to be applied.

For both the calibration fit and Rydberg fit, the χ^2 was lower than expected, which had to do with improperly matched uncertainties of H_r measurements. The same uncertainty was used for each angle measurement for both experiments, so adjusting the value for each measurement should cause the χ^2 to be closer to the degrees of freedom. Nevertheless, almost all residual error bars crossed the x-axis, so it can be concluded that the calibration and Rydberg fits both agree well with Eqs. 5 and 7. The uncertainties of those measurements likely could have been increased reasonably due to inconvenient laboratory conditions or measuring angles in the dark. For instance, the experimenter had to maneuver around the telescope in an awkward position to read the measurement. The experiment could be greatly improved with individually set angle measurement uncertainties and repeating the measurements of all angles to reduce the likelihood random error.

The calibration experiment can be completed with different gasses other than helium as a means of further study in the future. For example, calibration wavelengths of other known gas emission spectra could be utilized for the determination of the infinite mass Rydberg constant.

[1] R. DeSerio, *Visible spectrometer*, http://this.is.the.url.of.the.lab.manual.pdf (2022), Phy 4802L, Department of Physics, University of Florida.

[2] D. R. Paschotta, *Gas discharge lamps* (2021), URL https://www.rp-photonics.com/gas_discharge_lamps.html.

Appendix A: Comprehension Questions

1. C.Q.1

$$m\lambda = d[\sin(H_r - H_n) - \sin(H_i - H_n)]$$

$$m\lambda = d[\sin H_r \cos H_n - \cos H_r \sin H_n - \sin(H_i - H_n)]$$

$$m\lambda = d\cos H_n \sin H_r - d\sin H_n \cos H_r - d\sin(H_i - H_n)$$

Let $D_s = d\cos H_n$, $D_c = -d\sin H_n$, and $D_0 = -d\sin(H_i - H_n)$. Then it follows,

$$m\lambda = D_s \sin H_r + D_c \cos H_r + D_0$$

$$D_s^2 + D_c^2 = d^2\cos^2(H_n) + d^2\sin^2(H_n) = d^2$$

$$d = \sqrt{D_s^2 + D_c^2}$$

$$\frac{-d\sin H_n}{d\cos H_n} = \frac{D_c}{D_s}$$

$$\Rightarrow -\tan H_n = \frac{D_c}{D_s} \Rightarrow H_n = -\tan^{-1}\left(\frac{D_c}{D_s}\right)$$

$$\frac{D_0}{d} = -\sin\left(H_i - H_n\right) \Rightarrow \sin^{-1}\left(\frac{D_0}{d}\right) = -(H_i - H_n)$$

$$H_i = H_n - \sin^{-1}\left(\frac{D_0}{d}\right)$$

$$H_i = -\sin^{-1}\left(\frac{D_0}{\sqrt{D_s^2 + D_c^2}}\right) - \tan^{-1}\left(\frac{D_c}{D_s}\right)$$

2. C.Q.2

Via fitting parameters: d = 1657.292 (lines/nm), H_n = 209.521°, H_i = 218.892°

Measured: H_n = 209.516°, H_i = 218.913° Both the fitted and measured angles are similar to one part in a hundred.

3. C.Q.5

With the correction $\lambda/\lambda_m = n$ the Rydberg constant in a vacuum becomes 109690.9663 cm^{-1} which is a 31 cm^{-1} change to the fitted reduced mass Rydberg. In fact, the constant got smaller and closer to the reference value. Considering that the difference is greater than the uncertainty of the initial measurement of the Rydberg, this is significant in terms of the precision of the measurements.

	$[J_b^d]$		
	D_0	D_s	D_c
d	0	-0.870175	0.49274252
H_n	0	0.000297	0.000525059
H_i	-0.000612	0.000384	0.000475991

σ_d	$[\sigma_d^2]$		
0.235834076	0.055618	-5.1E-05	-8.89598E-06
0.000267845	-5.1E-05	7.17E-08	1.88974E-08
9.06659E-05	-8.9E-06	1.89E-08	8.22031E-09

FIG. 4: Jacobian of parameters with calculated parameter covariance matrix and corresponding uncertainties ← (C.Q.2)